Chemistry–A European Journal
Research Article
doi.org/10.1002/chem.202203289
Chemistry Europe
European Chemical Societies Publishing
www.chemeurj.org

Caging of a Strongly Pairing Fluorescent Thymidine Analog with Soft Nucleophiles

Juri Eyberg,[a] Mark Ringenberg,[a] and Clemens Richert*[a]

Abstract: Controlling the pairing strength of nucleobases in DNA through reactions with compounds found inside the cell is a formidable challenge. Here we report how a thiazolyl substituent turns a strongly pairing ethynylpyridone *C*-nucleoside into a reactive residue in oligonucleotides. The thiazolyl-bearing pyridone reacts with soft nucleophiles, such as glutathione, but not with hard nucleophiles like hydroxide or carbonate. The addition products pair much more weakly with adenine in a complementary strand than the starting material, and also change their fluorescence. This makes oligonucleotides containing the new deoxynucleoside interesting for controlled release. Due to its reactivity toward *N*, *P*, *S*, and *Se*-nucleophiles, and the visual signal accompanying chemical conversion, the fluorescent nucleotide reported here may also have applications in chemical biology, sensing and diagnostics.

Introduction

Reactive nucleosides are known as molecular tools for the investigation of mutations[1] and post-synthetic modifications of DNA strands in vitro or in vivo. Typical applications are probing,[2] crosslinking,[3] and the use as suicide inhibitors of enzymes.[4] Further, there are reactive nucleosides that are useful in synthesis and bioconjugation. For example, 'convertible nucleosides' have been described that react with nucleophiles like amines and thiols, producing a wide range of useful products.[5–10] Another group of reactive nucleosides contain bases with alkynyl substituents, including 5-ethynyluridine,[11] which acts as starting material for 1,3-dipolar cycloadditions with azides, resulting in crosslinking, labeling, or steps in the modular synthesis of complex target molecules.[11,12]

A special class of reactive compounds are 'caged' nucleosides.[13] These nucleosides transition to their active form only after a chemical reaction has been induced. A typical example is thymidine derivative **1** (Scheme 1).[14] Thymidine is locked or caged in its lactim form, preventing Watson-Crick base pairing with A, but, upon irradiation with UV light, the photolabile group is removed, and the active form of the nucleoside is released. The control over the base pairing status can be used to study biological processes.[15] While uncaging of nucleobases is frequently used on the oligonucleotide level, site-specific blocking or active caging of nucleosides of fully assembled strands is rare.

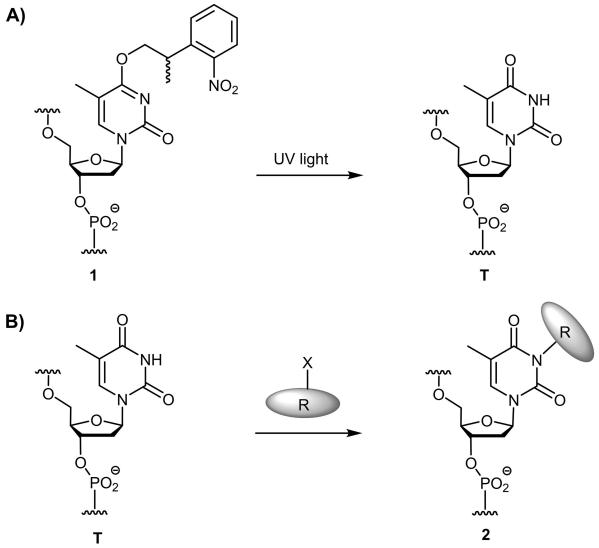

Scheme 1. Typical caging reactions. (A) Uncaging,[14] and (B) caging of a thymidine residue in an oligodeoxynucleotide.

Conceptually, caging of thymidine is not difficult to achieve (Scheme 1B). For example, derivatization of *N3* of T with a bulky group (**2**) or locking a lactim ether at *O4* can prevent base pairing. Achieving the necessary chemo- and regioselectivity on the oligonucleotide level is difficult, though. Instead, published examples achieve the destabilization of DNA duplexes through oxidation[16] or photochemical removal of a base surrogate.[17] In the first case, all guanines in the sequence were oxidized, and in the second case, a base analog with modest pairing strength had to be used, and the irradiation also induced strand cleavage. Reversible glyoxal caging[18] or acylation of the 2′-hydroxyl groups of RNA are known,[19,20] but more than one

[a] *J. Eyberg, Dr. M. Ringenberg, Prof. C. Richert*
Institute of Organic Chemistry
University of Stuttgart
70569 Stuttgart (Germany)
E-mail: lehrstuhl-2@oc.uni-stuttgart.de
Homepage: https://chip.chemie.uni-stuttgart.de/

Supporting information for this article is available on the WWW under https://doi.org/10.1002/chem.202203289

nucleoside was affected, and reagents were needed that are not abundant in living cells.

Neither of the published examples of reactive nucleosides involve a nucleoside with increased base pairing strength compared to the natural counterpart. Nor do the known caging reactions lead to a change of intrinsic fluorescence of the nucleoside undergoing the reaction. Also, to the best of our knowledge, base-selective caging of strongly pairing nucleosides with molecules found in the cell has not been reported previously.

We have recently reported *C*-nucleosides analogs of thymidine with an ethynylpyridone as nucleobase surrogate. Other work has focused on replacing deoxyadenosine with more strongly pairing analogs.[21] Our work included a deoxyuridine analog, dubbed E,[22] and the thymidine analog W shown in Figure 1.[23] Replacing thymidines in oligodeoxynucleotides with these *C*-nucleosides can increase the UV-melting point of the duplex with a complementary strand by up to 2.6 °C in the former case and up to 4.4 °C for the latter. Further, both E and W show excellent mismatch discrimination, resulting in drops in melting point opposite the 'wobble pair' partner G up to 20.5 °C. The increases in affinity and fidelity are attributed to the improved shape complementarity to adenine, with the ethynyl group well positioned to engage the CH fragment at the 2-position of the purine,[24,25] and inducing a steric clash when trying to pair with guanine. Exploiting these favorable pairing properties has been facilitated by the recent development of an optimized phosphoramidite building block for solid-phase synthesis.[26]

While ethynylpyridones have shown potential as antiviral drugs[27] and as monomers in chemical primer extension, where the activated monophosphate of W was found to be superior to its TMP counterpart,[28] there have been no reports on reactive versions of either E or W. This is why we decided to explore the properties of the new *C*-nucleosides Y and J (Figure 1) when we found them to possess reactivity. These new *C*-nucleosides feature substituents at the 3-position of the pyridone ring, corresponding to the 5-position of thymidine. The substituents chosen were the propynyl and the thiazolyl group, respectively, i.e. groups known to increase affinity for complementary strands at the 5-position of pyrimidines.[29–31] Here we report the synthesis of Y and J and reactions that they undergo, resulting in what may loosely be called 'caging', as it affects their base pairing properties.

Results and Discussion

The first nucleoside prepared was **3**, the immediate synthetic precursor to the deoxynucleoside form of Y. Scheme 2 shows the synthetic route chosen. It uses leaving groups at the 3- and 6-positions of the pyridone scaffold in order to achieve regioselective introduction of the different alkynyl groups, and three Pd-catalyzed cross couplings for the elaboration of the carbon framework. In the first step, nitropyridone **4** was *O*-benzylated to **5** under conditions that avoid *N*-alkylation, resulting in a yield of 97%. The protected aglycone was then employed in a Heck reaction with glycal **6**, which had been prepared via a known synthetic route.[22] The conditions for the Heck coupling had previously been optimized for *C*-nucleoside W,[23] and gave a similar yield in the present case. Silyl enol ether **7** was immediately desilylated to ketone **8**, which is also labile and was converted to nucleoside **9** by diastereoselective reduction. A yield of 79% over 3 steps was achieved for the glycosylation sequence, which is higher than that reported for Piv-protected W,[23] most probably because the benzyl protecting group is more stable and because the aglycone is more electron deficient than the methyl derivative.

In order to install a bromine substituent at the 3-position, nitropyridine **9** was converted to **10** in a Béchamp reduction. The reaction conditions were chosen to be mild to avoid a loss of benzyl protecting groups. The subsequent bromination with NBS then gave *C*-nucleoside **11** in 91% yield. Having prepared what is the 6-position in the final product for cross coupling, an iodo substituent was installed at the 3-position by diazotization followed by iodination. The resulting dihalide **12** constituted the key compound for the synthesis of both Y and J, and may also be used for the synthesis of other alkynylpyridone *C*-nucleosides in the future.

In the case of Y, **12** was converted to **3** in two consecutive Sonogashira reactions, using first propyne and then triisopropylsilyl acetylene as reaction partners. The two alkynyl residues were introduced chemoselectively by exploiting the difference in reactivity between the bromo and iodo substituents of **12** under cross coupling conditions. Debenzylation then gave the

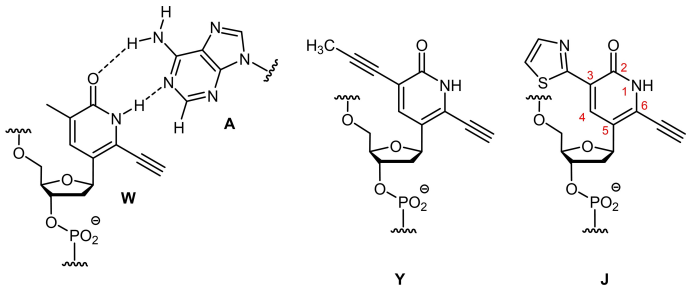

Figure 1. Structures of strongly-pairing ethynylpyridone *C*-nucleosides, including the known pyridone W,[23,26] shown as base pair with adenine (A), and the new derivatives Y and J, with numbering in the pyridone ring shown in red.

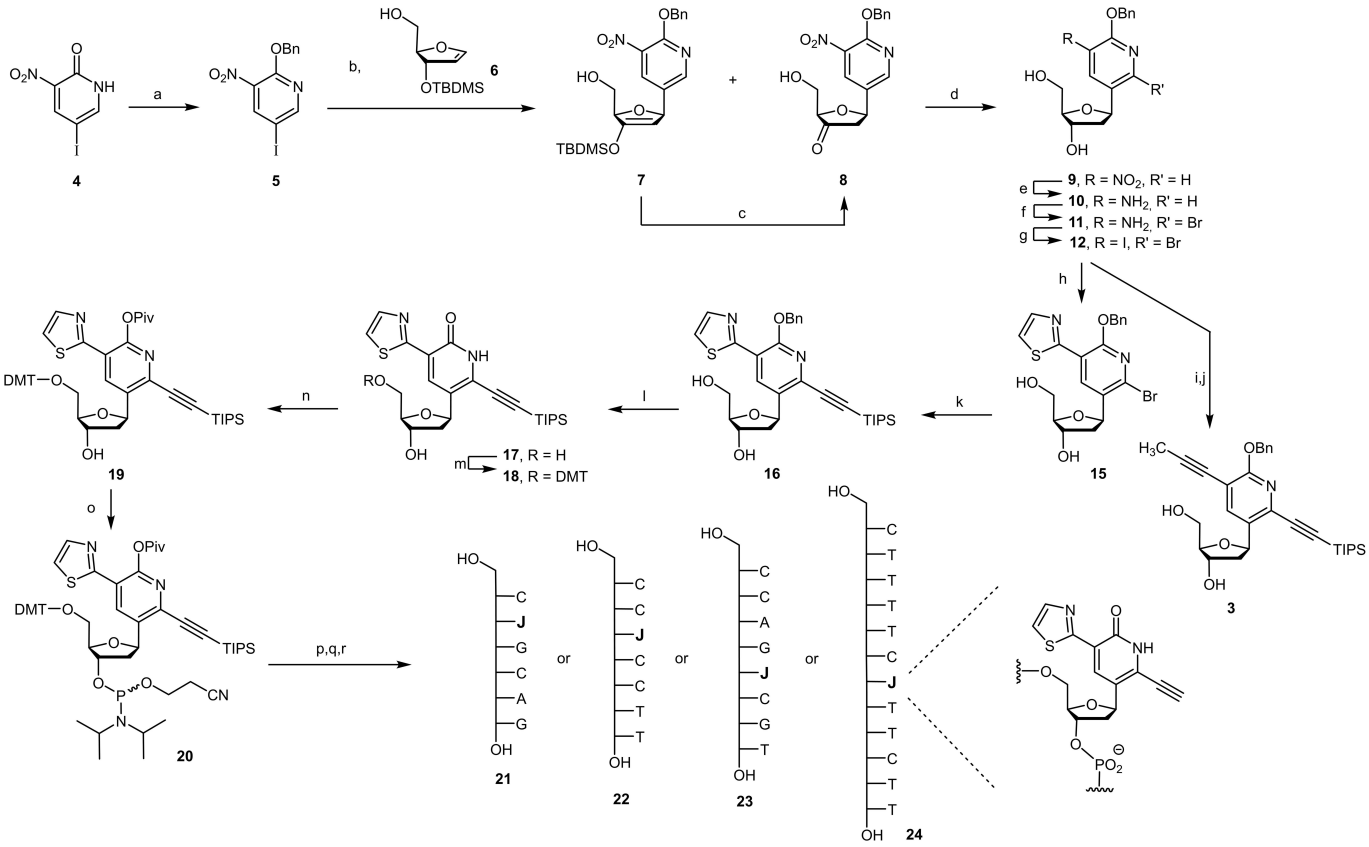

Scheme 2. Synthesis of dialkinyl *C*-nucleoside **3**, phosphoramidite **20**, and **J**-containing oligonucleotides. (a) BnBr, Ag_2CO_3, toluene, 80 °C, 97%; (b) **6**, $Pd(OAc)_2$, $P(PhF_5)_3$, Ag_2CO_3, CH_3CN; (c) 3 HF·NEt_3, THF; (d) $NaBH(OAc)_3$, AcOH, CH_3CN, 0 °C, 79% over 3 steps; (e) Fe, NH_4Cl, EtOH, 50 °C, 67%; (f) NBS, MeOH, CH_3CN, 0 °C, 91%; (g) 1. $NaNO_2$, HCl, H_2O, 0 °C; 2. KI, CH_3CN, H_2O, 52% over 2 steps; (h) 1. Ac_2O, pyridine; 2. 2-(tributylstannyl)thiazole, $[Pd(PPh_3)_2Cl_2]$, dioxane, 90 °C; 3. K_2CO_3, MeOH, 88% over 3 steps; (i) propyne, $Pd(PPh_3)_2Cl_2$, CuI, NEt_3, DMF, 91%; (j) triisopropylsilylacetylene, $Pd(PPh_3)_2Cl_2$, CuI, NEt_3, DMF, 80 °C, 74%; (k) triisopropylsilylacetylene, $[Pd(PPh_3)_2Cl_2]$, CuI, Et_3N, DMF, 80 °C, 91%; (l) TMS–Cl, NaI, CH_3CN, 41%; (m) DMT–Cl, DMAP, pyridine, 57%; (n) Piv-Cl, Et_3N, CH_3CN, 0 °C, 93%; (o) $(iPr_2N)_2P(OC_2H_4CN)$, DIPAT, CH_3CN, 97%; (p) solid-phase DNA synthesis cycles; (q) NH_4OH, 55 °C, (r) TBAF, THF. Abbreviations: Bn = benzyl, DIPAT = diisopropylammonium tetrazolide, DMAP = 4-dimethylaminopyridine, DMT = 4,4′-dimethoxytrityl, NBS = *N*-bromosuccinimide, Piv = pivaloyl, TBDMS = *tert*-butyldimethylsilyl, TIPS = triisopropylsilyl, TMS = trimethylsilyl.

desired *C*-nucleoside **13**, but the main product of the reaction was cyclized *C*-nucleoside **14** (Scheme 3), indicating that **13** is too reactive to be useful for employing it on the oligonucleotide level. Even under neutral conditions and at low temperature, **13** reacted to **14** in a 5-*endo-dig* cyclization. This reaction has also been reported for thymidine derivatives.[32] It changes the pattern of hydrogen bond acceptors/donors, thus interfering with Watson-Crick base pairing with adenine in a complementary strand.

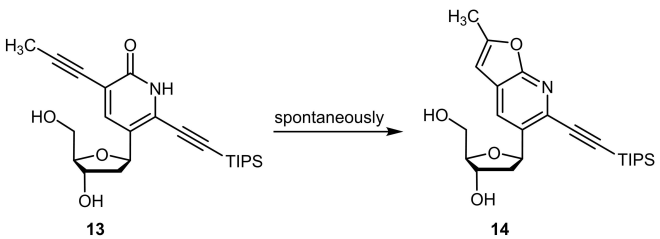

Scheme 3. Cyclization of diacetylide **13** to **14** lacking the hydrogen bond donor required for a thymidine analog.

Synthetically, the cyclization on the nucleoside level could be avoided by a change in the sequence of reactions, removing the TIPS protecting group first, followed by debenzylation. With this synthetic route, the phosphoramidite of Y was obtained successfully, and DNA solid phase synthesis was performed. When placing a residue of Y (instead of a thymidine) in a self-complementary DNA sequence, the UV-melting point of its duplex increased by up to 14.0 °C, but cyclization again occurred at elevated temperatures, even in neutral aqueous buffer. This level of reactivity was deemed problematic for applications in chemical biology or medicine, and Y was not pursued further. Instead, nucleoside J was elaborated, starting from **12** (Scheme 2). Here, a 5-*endo-dig* cyclization reaction was unlikely, and the more extended π-system promised additional stacking interactions with neighboring bases in double helices, as well as interesting optical and chemical properties. Other aromatic substituents, like phenyl[33] and pyrenyl[34,35] groups, at the 5-position of uracil can decrease the melting point of DNA and RNA duplexes, probably due to the lack of coplanarity in the biphenyl-like structure, but a thiazole ring linked via its

2-position does not possess hydrogens in the ortho positions, avoiding steric conflicts in a coplanar conformation.

Furanyl-, thiophenyl-, and oxazolyl- substituents at the 5-position of deoxyuridines show interesting fluorescence properties, but have a limited impact on duplex stability.[36–38] In contrast, the 5-(thiazol-2-yl)-2′-deoxyuridine residue[29] increases melting points of DNA/RNA duplexes by 1.7 °C per modification, which is close to the 1.6 °C per modification for the 5-propynyl group, found in the same study. The higher reactivity of the iodo substituent of **12** was used to introduce the thiazolyl residue via a Stille coupling, employing a commercially available reagent. To achieve high yields in the cross coupling, transient acetyl protection of the hydroxy groups was performed. After Stille coupling and deacetylation, **15** was obtained in 88% yield.

For the subsequent introduction of the triisopropyl (TIPS) protected acetylene, a Sonogashira coupling at 80 °C was used, giving **16** in 91% yield. In the next step, the benzyl protecting group had to be removed, as its deprotection after DNA synthesis was considered too risky. Since the alkynyl residue is labile under the strongly reducing conditions routinely used for debenzylation, a deprotection with in situ generated trimethylsilyl iodide was chosen, producing **17** in modest yield. An analytical sample was deprotected further to obtain the X-ray crystal structure and UV-Vis spectrum of the free nucleoside J shown in Figure 2. The X-ray structure confirmed that the desired β-anomer was obtained, and showed the coplanarity of the two aromatic rings. The extended π-system of J also manifested itself in a strong bathochromic shift of the longest wavelength absorption maximum, compared to that of thymidine, and its yellow color. Further details are provided in the Supporting Information.

The synthesis of the phosphoramidite building block of J proceeded via dimethoxytritylation of **17** to **18** and pivaloyl protection of the nucleobase of the latter to **19**. The Piv group was chosen, as it can be easily removed during the cleavage of oligonucleotides from controlled-glass solid support. Phosphitylation then produced **20**, which was used in subsequent solid-phase DNA syntheses.

With phosphoramidite **20**, oligodeoxynucleotides **21**–**24** were synthesized (Scheme 2). To avoid having to fill the void volumes of a fifth channel of our DNA synthesizer, the coupling of the new building block was performed manually. Three of the sequences (**21**, **22** and **24**) were chosen to allow for comparison with thymidine derivatives described earlier.[22,23,30] Sequence **23** was chosen to study mismatch discrimination, and to compare the new base pair with a G:C base pair. After solid phase DNA synthesis and cleavage from the solid support with aqueous ammonia, the TIPS groups on J were removed with TBAF, followed by desalting. After RP HPLC, MALDI spectra and the chromatogram showed the desired ODNs in high purity and yields.

However, after lyophilization of the product fractions from triethylammonium acetate (TEAA) buffer, a significant part of the desired oligonucleotides was found to have reacted with the triethylamine (Scheme 4). The Michael acceptor-like reactivity at the 3-position of J was apparently high enough to allow for addition at the high salt concentrations of lyophilization. Other addition reactions have been reported for ethynyl-substituted nucleosides,[39] but in those cases, strongly basic conditions and elevated temperatures were required for conversion.

In a subsequent HPLC step with ammonium bicarbonate buffer, **24** and **25** were separated, and no addition products were found after lyophilization, confirming that hard nucleophiles, including ammonia and carbonate, do not readily react with the ethynylpyridone. As a consequence, the subsequent

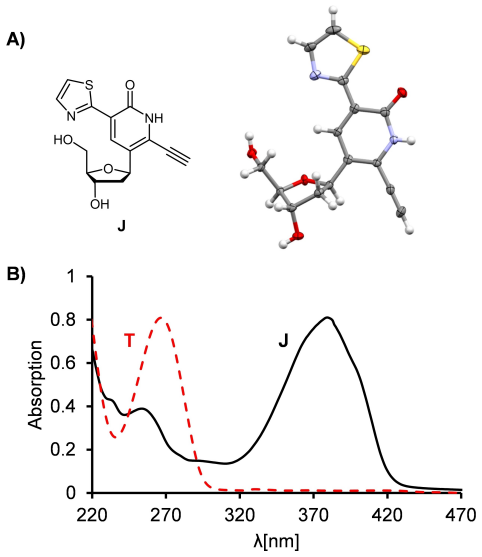

Figure 2. Structure and absorption spectra of free nucleoside J. A) X-ray crystal structure, and B) UV-Vis spectra of 0.08 mM solutions of J and thymidine in MeOH.

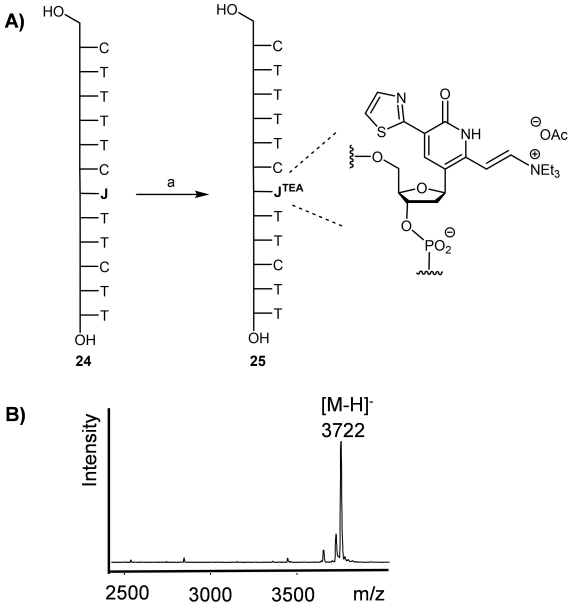

Scheme 4. Reaction of DNA strand **24** with triethylamine. A) Reaction scheme, (a) lyophilization from 0.1 M triethylammonium acetate buffer, pH 7.0; B) MALDI-TOF mass spectrum of product **25**.

syntheses of J-containing oligonucleotides used HPLC purification with ammonium bicarbonate buffer, which prevented 'caging' in all cases studied. Another nucleophile leading to detectable addition was trihydroxy acetophenone, though, our preferred matrix for MALDI-TOF mass spectrometry.[40] Other matrix systems containing soft nucleophiles also gave the corresponding matrix adducts in the spectra obtained by the usual sample preparation, which includes evaporation and laser irradiation to generate ions in the source of the spectrometer.

The addition product from the reaction with triethylamine (**25**) showed a red-shift in its fluorescence, compared with **24**, indicating that conversion can be monitored visually. This encouraged us further to study the reactivity of the new *C*-nucleoside. First, reactions were performed with the free nucleoside J, which were analyzed by NMR spectroscopy.

Two new peaks in the olefinic range appeared in the ^{1}H NMR spectrum during the reaction with TEA (see Supporting Information). The data from 2D NMR spectra was in agreement with the structure shown in the expansion of Scheme 4A. The formation of vinyl ammonium salts in reactions with tertiary amines with alkynes is known for acetylene,[40] but has, to the best of our knowledge, not been reported for deoxynucleosides like J.

We then studied the stability of the A:J base pair in UV melting experiments. The J-containing strands were found to remain unreactive in phosphate buffer, even after several heating and cooling cycles. Figure 3 shows the melting curves of **24** and its complementary DNA strand (**26**), as well as those of its unmodified DNA counterpart (**27**) and that for the duplex with reaction product **25**.

In the case of dodecamer **24**, the melting point was 5.0 °C higher than that of the unmodified counterpart. Compared to known ethynylmethylpyridone W,[23] this is an additional melting point increase of 1.2 °C and the highest value for our *C*-nucleosides to date. We also noted the low-temperature transition in the melting curve of the duplex with **24** typical for triplex formation.[42] This is in line with observations for thymidine analogs studied earlier using, the current sequence capable of triplex formation,[43,22] and suggests that the thiazole ring does not interfere with Hoogsteen base pairing in the major groove.

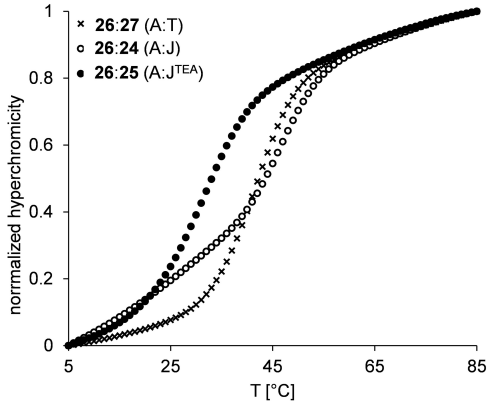

Figure 3. A) UV-melting curves of DNA dodecamer duplexes with natural A:T, A:J or A:J^{TEA} base pairs. Conditions: 1.6 μM strands, 10 mM phosphate buffer, pH 7.0, 1 M NaCl, measured at 260 nm.

For self-complementary sequence **21**, which can form two A:J base pairs upon hybridization, an increase in T_m of 12.8 °C over that of the control duplex was measured (Table 1). In contrast, with TEA adduct **25**, the duplex melting point was 17 °C lower than that with J-containing **24**, even though only a single base had been converted, demonstrating just how strongly the base pairing properties of J can be tuned by addition reactions. The stability of the A:J base pair was then compared to that of the C:G base pair, using sequence **23** and unmodified control strands. Compared to the A:T-containing duplex, the G:C base pair gave +6.0 °C in ΔT_m, whereas the A:J base pair gave +7.0 °C, again confirming how strongly duplex stabilizing J is. Octamer **23** was also used to study mismatch discrimination (Table 2). For mismatched bases opposite J, the drop in T_m was ≥12 °C in each case, whereas opposite T, a G, causing a wobble base pair, gave a ΔT_m of 9.8 °C. So, J is

Table 1. UV melting points of DNA duplexes with A:J base pairs or their control duplexes, containing canonical A:T or G:C base pairs.

Strands	T_m [°C][a]	ΔT_m [°C][b]
3′-GAAAAGAAAGAA-5′ (**26**)		
5′-CTTTTCTTTCTT-3′ (**27**)	43.0	
5′-CTTTTCJTTCTT-3′ (**24**)	48.0	+5.0
5′-CTTTTC^{TEA}JTTCTT-3′ (**25**)	31.0	−12.0
(5′-CTGCAG-3′)$_2$ (**28**)	25.5	
(5′-CJGCAG-3′)$_2$ (**21**)	38.3	+12.8
3′-GGACCTT-5′ (**29**)		
5′-CCTCCTT-3 (**30**)	27.0	
5′-CCJCCTT-3 (**22**)	33.9	+6.9
3′-GGTCAGCA-5′ (**31**)		
5′-CCAGTCGT-3′ (**32**)	40.0	
5′-CCAGJCGT-3′ (**23**)	47.0	+7.0
3′-GGTCCGCA-5′ (**33**)		
5′-CCAGGCGT-3′ (**34**)	46.0	+6.0

[a] Average of four curves. Conditions: 1.6 μM to 6.4 μM strands, depending on the sequence chosen, 10 mM phosphate buffer, pH 7.0, 1 M NaCl; [b] To A:T control duplex. [c] ^{TEA}J = triethylammonium adduct of J.

Table 2. UV melting points of DNA octamer duplexes with T or J facing A or a mismatched nucleobase.

Strands	base pairing	T_m [°C][a]	ΔT_m [°C][b]
5′- CCAGTCGT-3′ (**32**)			
3′- GGTCAGCA-5′ (**31**)	T:A	40.3	
3′- GGTCTGCA-5′ (**35**)	T:T	18.8	−21.5
3′- GGTCCGCA-5′ (**33**)	T:C	15.3	−25.0
3′- GGTCGGCA-5′ (**36**)	T:G	30.5	−9.8
5′- CCAGJCGT-3′ (**23**)			
3′- GGTCAGCA-5′ (**31**)	J:A	47.0	
3′- GGTCTGCA-5′ (**35**)	J:T	18.5	−28.5
3′- GGTCCGCA-5′ (**33**)	J:C	24.5	−22.5
3′- GGTCGGCA-5′ (**36**)	J:G	35.0	−12.0

[a] Average of four curves; [b] To T_m of fully matched duplex. Conditions: 3.2 μM strands, 10 mM phosphate buffer, pH 7.0, 1 M NaCl.

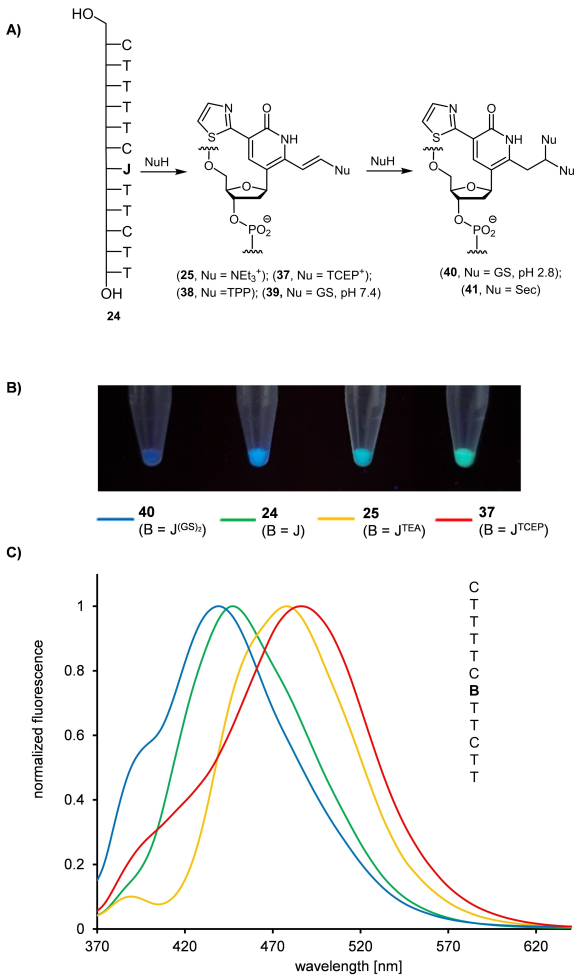

Figure 4. Addition of nucleophiles to **24** and the resulting change in fluorescence. A) Reaction scheme; B) photographs of reaction solutions under UV light (λ_{ex} = 366 nm, 10.7 μM strand concentration); C) Normalized emission spectra of the diluted solutions (0.1 μM, λ_{ex} = 345 nm). Abbreviations: TCEP, tris(2-carboxyethyl)phosphine; TEA, triethylamine; TPP, thiamine pyrophosphate; Sec, selenocysteine.

Table 3. Reaction of J with different nucleophiles and its influence on the emission wavelength; TEAA = triethylammonium acetate.

Nucleophile	Reaction conditions	Product	λ_{em} [nm]
–	–	**24**	447
tris(2-carboxyethyl) phosphine	10.7 μM 24, 125 mM NuH, pH 7.0, 25 °C, 16 h	**37**	486
Triethylamine	Lyophilization of 24 from TEAA buffer (0.1 M, pH 7.0)	**25**	478
Thiamine pyrophosphate	10.7 μM 24, 125 mM NuH, 37 °C, 16 h	**38**	455
Glutathione	10.7 μM 24, 125 mM NuH, pH 2.8, 37 °C, 16 h	**40**	439
Selenocysteine	10.7 μM 24, 125 mM NuH, pH 4.6, 37 °C, 16 h	**41**	424

superior to T in both affinity for the complementary base and in fidelity.

This encouraged us to study properties of J that are useful for practical applications. As mentioned above, Michael-type addition did not occur with hard nucleophiles, like hydroxide or ammonia, but with soft nucleophiles. To better understand the scope of the addition, other nucleophiles were tested using the reaction of Figure 4A. Here, oligonucleotide **24** was allowed to react, and its conversion was monitored by MALDI-TOF mass spectrometry, as well as fluorescence spectroscopy. In the event, besides TEA; tris(2-carboxyethyl)phosphine (TCEP), thiamine pyrophosphate (TPP), glutathione, and selenocysteine were found to react. The reaction conditions are given in Table 3.

A single addition led to a red-shift of the emission by up to 39 nm without loss of the intense fluorescence (Figure 4). For ammonium or phosphonium-terminated olefinic products, a push-pull chromophore is obtained, with strong absorption and emission. For thiol- or a selenol-containing nucleophiles glutathione and selenocystein, a double addition was inducable under acidic conditions, where the thiazole ring is protonated and the Michael acceptor moiety is more reactive as electrophile. In the latter case, the vinylic product of the first addition step is converted to a saturated system, reducing the size of the π-system. This, in turn, manifests itself in a hypsochromic shift of the main fluorescence band. For selenocysteine, the shift was 23 nm compared to that of **24**, i.e. 62 nm blue-shifted compared to the addition product with TCEP.

To get a better photophysical understanding for the addition products of triethylamine and glutathione, as well as free nucleoside J, fluorescence quantum yields were determined. Details are given in Table S3 of the Supporting Information. The quantum yields ranged from 60% for J itself to 25% for the double addition product of glutathione. This compares favorably with 5-thiazolyl-2′-deoxyuridine, for which the fluorescence quantum yield is known to be below 1%.[36] Together, this data suggests that J residues in oligonucleotides can serve as molecular sensors,[44] complementing existing systems for the detection of soft nucleophiles.[45]

Each nucleophile gives a product with characteristic emission spectrum (Figure 4C), and often the differences in color that can be observed with the naked eye (Figure 4B). Finally, exploratory experiments were performed to obtain a proof-of-principle result for use of the addition reaction in programmed release of nucleic acids. This application makes use of the exceptional change in affinity for a complementary base upon reaction with glutathione, an important redox agent inside the cell. We reasoned that upon delivery of a duplex with oligonucleotides containing J into a cell, the addition reaction with this soft nucleophile could weaken the double helix enough to induce the release of the complementary strand.

The exploratory experiments were performed with **23** in duplex with complementary strand **31** (Figure 5A). Reaction conditions were chosen to mimic physiological conditions. The reaction was monitored by fluorescence spectroscopy and formation of the glutathione adduct was confirmed by MALDI-TOF MS (Figure 5B). At pH 7.4, one glutathione molecule was

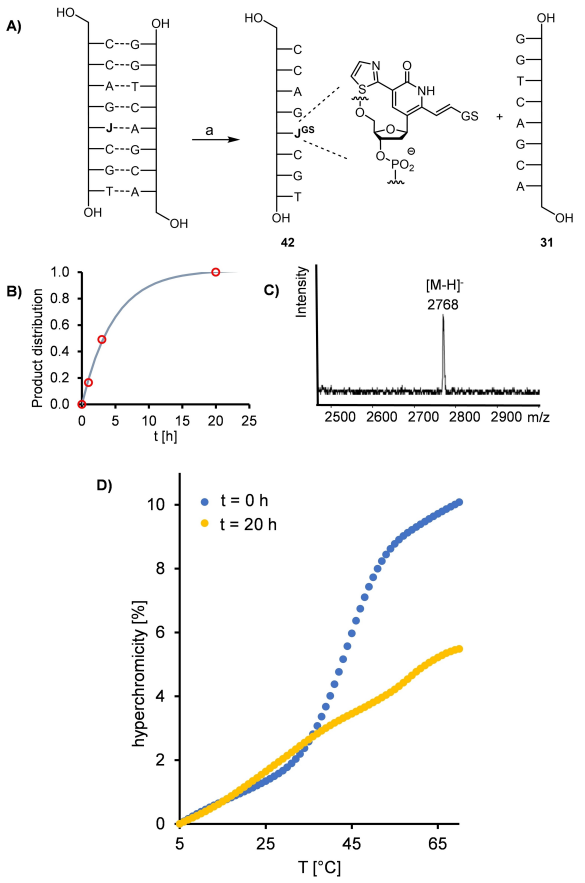

Figure 5. Reaction of the J-containing DNA duplex (**23**/**31**) with glutathione leads to a release of the complementary strand (**31**). Conditions: 1.6 μM strands, 5 mM glutathione, PBS buffer, pH 7.4, 37 °C. A) Equation; B) Kinetics, monitored by fluorescence at 500 nm; C) MALDI-TOF mass spectrum confirming formation of the addition product after 20 h; D) UV melting curves before and after the reaction with glutathione.

added to **23** with a half-life time of 3.3 h. To demonstrate the effect on the duplex, UV melting curves were measured prior to and after the reaction (Figure 5D). Before the reaction with glutathione, the melting point was 44.0 °C, but no sigmoidal transition was observed afterwards. In a control assay with unmodified strands the melting point remained the same after exposure to glutathione. The decrease in the melting point was larger than for the TEA adduct, probably because glutathione causes more steric hinderance and does not give a cationic adduct, whose positive charge provides a modest level of Coulombic attraction. This data confirms that 'caging' J with glutathione destabilizes the duplex to an extent that releases the complementary strand.

It is interesting to ask how the unusual reactivity of J may be used in chemical biology. It is reasonable to assume that strand-release effects can be achieved for longer cargo strands than the short complementary strand employed in our model assay. In order to have a strong enough effect upon reaction with intracellular nucleophiles, carrier strands with several J residues may be used. The cargo strands may be therapeutically active oligonucleotides like antisense or antigen oligonucleotides or possibly mRNAs hybridized to multiple carrier oligonucleotides.[46] An efficient release process appears realistic because the concentration of free glutathione is low outside the cell, but it is abundant inside the cell,[47] so that rapid intracellular release by addition to J is conceivable.

Finally, we asked what the molecular basis of the strong effects of J on duplex stability and its high reactivity are. For this, DFT calculations were performed on J and its unreactive counterpart E (Figure 6). The structure obtained for J was in agreement with the X-ray crystal structure, showing a coplanar arrangement of all parts of the aglycone, suitable for extensive stacking interactions, as well as the properly positioned ethynyl group for interacting with the H2-region of adenine.[24,48]

Insight into the high reactivity of J in Michael-type addition reactions were obtained from calculated LUMO energies. Figure 6B shows that both J and E have large enough atom coefficients at the distal carbon of the ethynyl group for HOMO-LUMO interactions in the transition state of the addition of a soft nucleophile. However, the LUMO of J is approx. 0.4 eV lower in energy than that of E, explaining why it is much more

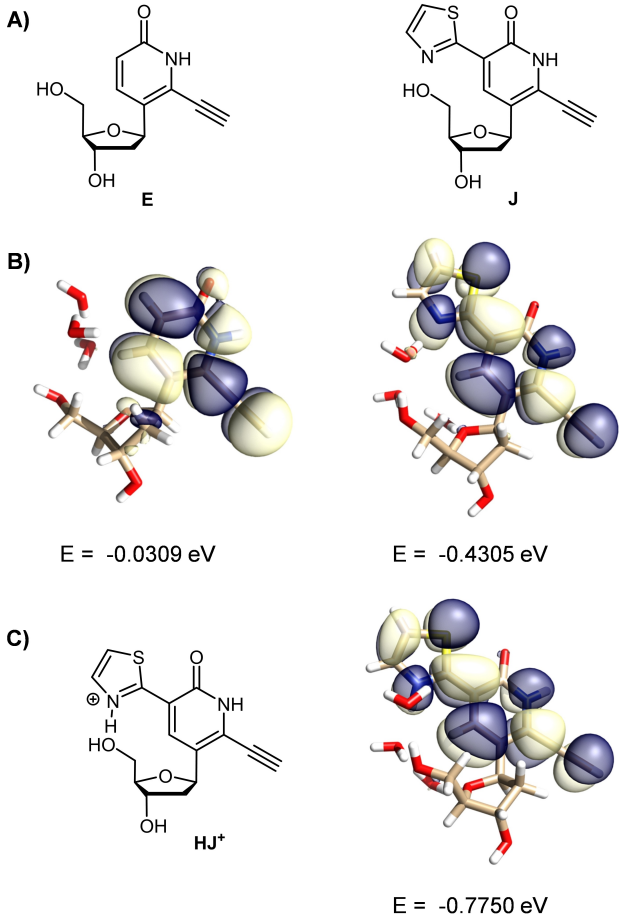

Figure 6. Results of DFT calculations for E and J. A) Structures of the nucleosides. B) Calculated LUMO for either of the nucleobases, as obtained with the wB97X functional at the def2-TZVP level in the presence of three water molecules. Below each nucleoside, the corresponding LUMO energies are given in electron volts. C) Calculated LUMO and LUMO energy of protonated J. Calculations and visualizations were performed with ORCA 5.0.1.[49]

reactive than the parent ethynylpyridone lacking the thiazole substituent. Since the thiazole ring is not a strongly electron withdrawing substituent, the larger π-system, with the higher number of MOs is a likely explanation. Perhaps more importantly, the thiazole ring can be protonated, turning it into a more strongly electron-withdrawing, cationic group. Calculations for the protonated form of J gave an approx. 0.7 eV lower LUMO energy than for E (see Table S3 in the Supporting Information), in agreement with this assumption.

Conclusions

The results presented here show that placing a thiazole ring at the 3-position of an ethynylpyridone *C*-nucleoside increases base pairing strength with adenine to a level above that for C:G base pairs. Further, it endows the base analog with properties that are both fascinating and potentially useful. A reactive nucleoside that changes its pairing properties upon undergoing 1,4-additions under mild conditions can be expected to find practical applications, particularly when it "reports" the change in structure through a change in its fluorescence signature. Besides intracellular release of cargo strands from duplexes, the practical applications may include the specific detection of nucleophiles and the unfolding of DNA nanostructures induced by a chemical trigger.

Experimental Section

Detailed protocols and additional experimental data, together with data on DFT calculations, can be found in the Supporting Information (SI).

DNA synthesis: The oligonucleotides containing J were synthesized on 1 μmol scale on long-chain alkylamine controlled-pore glass (cpg), using an H-2 synthesizer (K&A Laborgeräte, Schaafheim, Germany). Chain assembly cycles for unmodified nucleotides followed the recommendations of the manufacturer, whereas phosphoramidite **20** (27 mg, 25 μmol), was directly dissolved in activator solution (0.25 M 4,5-dicyanoimidazole in acetonitrile, 0.3 mL), and the resulting solution was added to the cpg, followed by mixing on a horizontal shaker for 1 h. After capping and oxidation, the remainder of the sequence was again assembled automatically. Deprotection and release from the support used aqueous ammonia (25%, 1 mL) for 16 h at 55 °C. After lyophilization, 1 M tetra-*n*-butylammonium fluoride (TBAF) solution in THF (0.5 mL) and water (20 μL) was added, and the solution was shaken for 5 h at 25 °C, followed by addition of triethylammonium acetate buffer (1 M, 0.5 mL), evaporation and chromatographic purification.

Crystal structure determination: Deposition Number 2220330 contains the supplementary crystallographic data for this paper. These data are provided free of charge by the joint Cambridge Crystallographic Data Centre and Fachinformationszentrum Karlsruhe Access Structures service.

Acknowledgements

The authors thank Prof. H.-A. Wagenknecht (KIT, Karlsruhe) for providing access to fluorescence spectrometers and instructions, Dr. W. Frey for X-ray analysis, D. Dittrich for measuring UV-VIS spectra, D. Göhringer for technical assistance, J. Han, Dr. F. Rami, T. Berking, Dr. B. Miehlich for discussions, and Deutsche Forschungsgemeinschaft (DFG) grant RI 1063/18-1 and Volkswagen Foundation (grant Az 92 768) for financial support. Open Access funding enabled and organized by Projekt DEAL.

Conflict of Interest

The authors declare no conflict of interest.

Data Availability Statement

The data that support the findings of this study are available in the supplementary material of this article.

Keywords: caging · DNA · nucleosides · nucleotides · reporters

[1] C. You, Y. Wang, *Nat. Protoc.* **2015**, *10*, 1389–1406.
[2] W. Dai, A. Li, N. J. Yu, T. Nguyen, R. W. Leach, M. Wühr, R. E. Kleiner, *Nat. Chem. Biol.* **2021**, *17*, 1178–1187.
[3] C. Prestinari, C. Richert, *Chem. Commun.* **2011**, *47*, 10824.
[4] W. A. Hartgers, R. F. de Boer, M. J. Wanner, G. J. Koomen, *Nucleosides Nucleotides Nucleic Acids* **1992**, *11*, 1325–1332.
[5] H. Wang, I. D. Kozekov, T. M. Harris, C. J. Rizzo, *J. Am. Chem. Soc.* **2003**, *125*, 5687–5700.
[6] C. R. Allerson, S. L. Chen, G. L. Verdine, *J. Am. Chem. Soc.* **1997**, *119*, 7423–7433.
[7] A. M. MacMillan, G. L. Verdine, *J. Org. Chem.* **1990**, *55*, 5931–5933.
[8] S. Bae, M. K. Lakshman, *J. Am. Chem. Soc.* **2007**, *129*, 782–789.
[9] Y. Z. Xu, Q. Zheng, P. F. Swann, *J. Org. Chem.* **1992**, *57*, 3839–3845.
[10] U. Ghanty, T. Wang, R. M. Kohli, *Angew. Chem. Int. Ed.* **2020**, *59*, 11312–11315; *Angew. Chem.* **2020**, *132*, 11408–11411.
[11] D. A. Reid, P. J. Reed, J. C. M. Schlachetzki, I. I. Nitulescu, G. Chou, E. C. Tsui, J. R. Jones, S. Chandran, A. T. Lu, C. A. McClain, J. H. Ooi, T.-W. Wang, A. J. Lana, S. B. Linker, A. S. Ricciardulli, S. Lau, S. T. Schafer, S. Horvath, J. R. Dixon, N. Hah, C. K. Glass, F. H. Gage, *Science* **2021**, *372*, 91–94.
[12] D. Perrone, E. Marchesi, L. Preti, M. L. Navacchia, *Molecules* **2021**, *26*, 3100.
[13] X. Tang, J. Zhang, J. Sun, Y. Wang, J. Wu, L. Zhang, *Org. Biomol. Chem.* **2013**, *11*, 7814.
[14] L. Kröck, A. Heckel, *Angew. Chem. Int. Ed.* **2005**, *44*, 471–473; *Angew. Chem.* **2005**, *117*, 475–477.
[15] L. Yang, I. J. Dmochowski, *Molecules* **2021**, *26*,1481.
[16] S. Jiranusornkul, C. A. Laughton, *J. R. Soc. Interface.* **2008**, *5*, 191–198.
[17] C. Crey-Desbiolles, *Nucleic Acids Res.* **2005**, *33*, 1532–1543.
[18] S. D. Knutson, A. A. Sanford, C. S. Swenson, M. M. Korn, B. A. Manuel, J. M. Heemstra, *J. Am. Chem. Soc.* **2020**, *142*, 17766–17781.
[19] A. Kadina, A. M. Kietrys, E. T. Kool, *Angew. Chem.* **2018**, *130*, 3113–3117; *Angew. Chem. Int. Ed.* **2018**, *57*, 3059–3063.
[20] W. A. Velema, A. M. Kietrys, E. T. Kool, *J. Am. Chem. Soc.* **2018**, *140*, 3491–3495.
[21] F. Seela, G. Becher, *Nucleic Acids Res.* **2001**, *29*, 2069–2078.].
[22] M. Minuth, C. Richert, *Angew. Chem.* **2013**, *125*, 11074–11077; *Angew. Chem. Int. Ed.* **2013**, *52*, 10874–10877.
[23] T. J. Walter, C. Richert, *Nucleic Acids Res.* **2018**, *46*, 8069–8078.
[24] A. Halder, A. Datta, D. Bhattacharyya, A. Mitra, *J. Phys. Chem. B* **2014**, *118*, 6586–6596.
[25] M. Chawlaa, S. Gorleb, A. R. Shaikha, R. Olivac, L. Cavallo, *Comp. Struc. Biotech. J.* **2021**, *19*, 1312–1324.
[26] J. Eyberg, D. Göhringer, A. Salihovic, C. Richert, *Eur. J. Org. Chem.* **2022**, e202200611.
[27] J. Han, C. Funk, J. Eyberg, S. Bailer, C. Richert, *Chem. Biodiversity* **2021**, *18*, e2000937.
[28] J. Han, E. Kervio, C. Richert, *Chem. Eur. J.* **2021**, *27*, 15918–15921.

[29] R. W. Wagner, M. D. Matteucci, J. G. Lewis, A. J. Gutierrez, C. Moulds, B. C. Froehler, *Science* **1993**, *260*, 1510–1513.
[30] T. Kottysch, C. Ahlborn, F. Brotzel, C. Richert, *Chem. Eur. J.* **2004**, *10*, 4017–4028.
[31] A. J. Gutierrez, T. J. Terhorst, M. D. Matteucci, B. C. Froehler, *J. Am. Chem. Soc.* **1994**, *116*, 5540–5544.
[32] C. J. Yu, H. Yowanto, Y. Wan, T. J. Meade, Y. Chong, M. Strong, L. H. Donilon, J. F. Kayyem, M. Gozin, G. F. Blackburn, *J. Am. Chem. Soc.* **2000**, *122*, 6767–6768.
[33] P. Kumar, M. Hornum, L. J. Nielsen, G. Enderlin, N. K. Andersen, C. Len, G. Hervé, G. Sartori, P. Nielsen, *J. Org. Chem.* **2014**, *79*, 2854–2863.
[34] C. Wanninger-Weiß, H.-A. Wagenknecht, *Eur. J. Org. Chem.* **2008**, *2008*, 64–71.
[35] J. Frommer, B. Karg, K. Weisz, S. Müller, *Org. Biomol. Chem.* **2018**, *16*, 7663–7673.
[36] N. J. Greco, Y. Tor, *J. Am. Chem. Soc.* **2005**, *127*, 10784–10785.
[37] N. J. Greco, Y. Tor, *Tetrahedron* **2007**, *63*, 3515–3527.
[38] M. S. Noé, R. W. Sinkeldam, Y. Tor, *J. Org. Chem.* **2013**, *78*, 8123–8128.
[39] S. A. Ingale, H. Mei, P. Leonard, F. Seela, *J. Org. Chem.* **2013**, *78*, 11271–11282.
[40] U. Pieles, W. Zürcher, M. Schär, H. E. Moser, *Nucleic Acids Res.* **1993**, *21*, 3191–3196.
[41] W. Reppe, *Experientia* **1949**, *5*, 93–110.
[42] N. T. Thuong, C. Hélène, *Angew. Chem. Int. Ed. Engl.* **1993**, *32*, 666–690.
[43] K. Ryan, E. T. Kool, *Chem. Biol.* **1998**, *5*, 59–67.
[44] N. Arndt, H. D. N. Tran, R. Zhang, Z. P. Xu, H. T. Ta, *Adv. Sci.* **2020**, *7*, 2001476.
[45] X. Jia, J. Li, E. Wang, *Chem. Eur. J.* **2012**, *18*, 13494–13500.
[46] V. Damakoudi, T. Feldner, E. Dilji, A. Belkin, C. Richert, *ChemBioChem* **2020**, *22*, 924–930.
[47] G. Wu, Y.-Z. Fang, S. Yang, J. R. Lupton, N. D. Turner, *J. Nutr.* **2004**, *134*, 489–492.
[48] D. J. Gibson, T. van Mourik, *Chem. Phys. Lett.* **2017**, *668*, 7–13.
[49] F. Neese, *WIREs Comput. Mol. Sci.* **2012**, *2*, 73–78.

Manuscript received: October 20, 2022
Accepted manuscript online: November 17, 2022
Version of record online: December 12, 2022